Electronic Supplementary Information : Photo-sensitizing thin-film ferroelectric oxides using materials databases and high-throughput calculations

Jose J. Plata,[1] Javier Amaya Suárez,[1] Santiago Cuesta-López,[2] Antonio M. Márquez,[1] and Javier Fdez Sanz[1]

[1] *Departamento de Química Física, Universidad de Sevilla, Seville, Spain*[*]

[2] *International Center in Advanced Materials and raw materials of Castilla y Leon, León, Spain*

(Dated: November 20, 2019)

Abstract

Conventional solar cell efficiency is usually limited by the Shockley-Queisser limit. This is not the case, however, for ferroelectric materials, which present a spontaneous electric polarization that is responsible for their bulk photovoltaic effect. Even so, most ferroelectric oxides exhibit large band gaps, reducing the amount of solar energy that can be harvested. In this work, a high-throughput approach to tune the electronic properties of thin-film ferroelectric oxides is presented. Materials databases were systematically used to find substrates for the epitaxial growth of $KNbO_3$ thin-films, using topological and stability filters. Interface models were built and their electronic and optical properties were predicted. Strain and substrate-thin-film band interaction effects were examined in detail, in order to understand the interaction between both materials. We found substrates that significantly reduce the $KNbO_3$ band gap, maintain $KNbO_3$ polarization, and potentially present the right band alignment, favoring the electron injection in the substrate/electrode. This methodology can be easily applied to other ferroelectric oxides, optimizing their band gaps and accelerating the development of new ferroelectric-based solar cells.

[*] jplata@us.es

S1. SUPERLATTICE CONSTRUCTION

In order to build all the surfaces with an area nA, the primitive surface vectors, **a** and **b**, are transformed in the superlattice surface vectors, **u** and **v**, using transformation matrices [1],

$$\begin{pmatrix} \mathbf{u} \\ \mathbf{v} \end{pmatrix} = \begin{pmatrix} i & j \\ 0 & m \end{pmatrix} \begin{pmatrix} \mathbf{a} \\ \mathbf{b} \end{pmatrix}, \tag{1}$$

where i, j and m are integers, and

$$i \cdot m = n, \tag{2}$$

$$i, m > 0, \tag{3}$$

$$0 \leq j \leq m - 1. \tag{4}$$

S2. $KNbO_3$ BULK BENCHMARK

TABLE S1. Lattice parameters a and c, ratio c/a, and indirect ($M \rightarrow \Gamma$) band gap, E_g, for tetragonal $KNbO_3$.

	LDA	PBEsol	PBE+U	HSE06-30	HSE06	exp.
a	3.945 [2]	3.969 [2]	3.998	-	-	3.997 [3]
c	3.989 [2]	4.058 [2]	4.022	-	-	4.063 [3]
c/a	1.011 [2]	1.022 [2]	1.006	-	-	1.017 [3]
E_g	1.40,1.50 [4, 5]	-	1.75	3.23 [2]	2.66 [4]	3.08,3.30 [6, 7]

S3. $KNbO_3$ BAND STRUCTURE

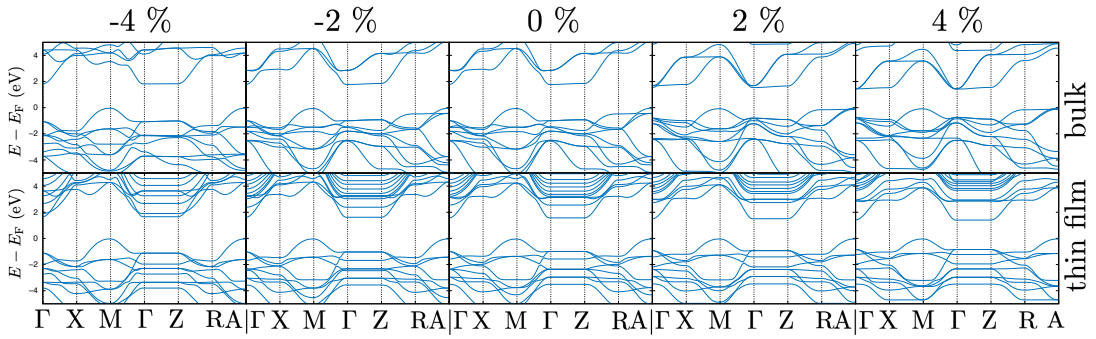

FIG. S1. Band structure for $KNbO_3$ bulk (top panels) and thin-film (bottom panels) applying compressive (negative) and tensile (positive) strain.

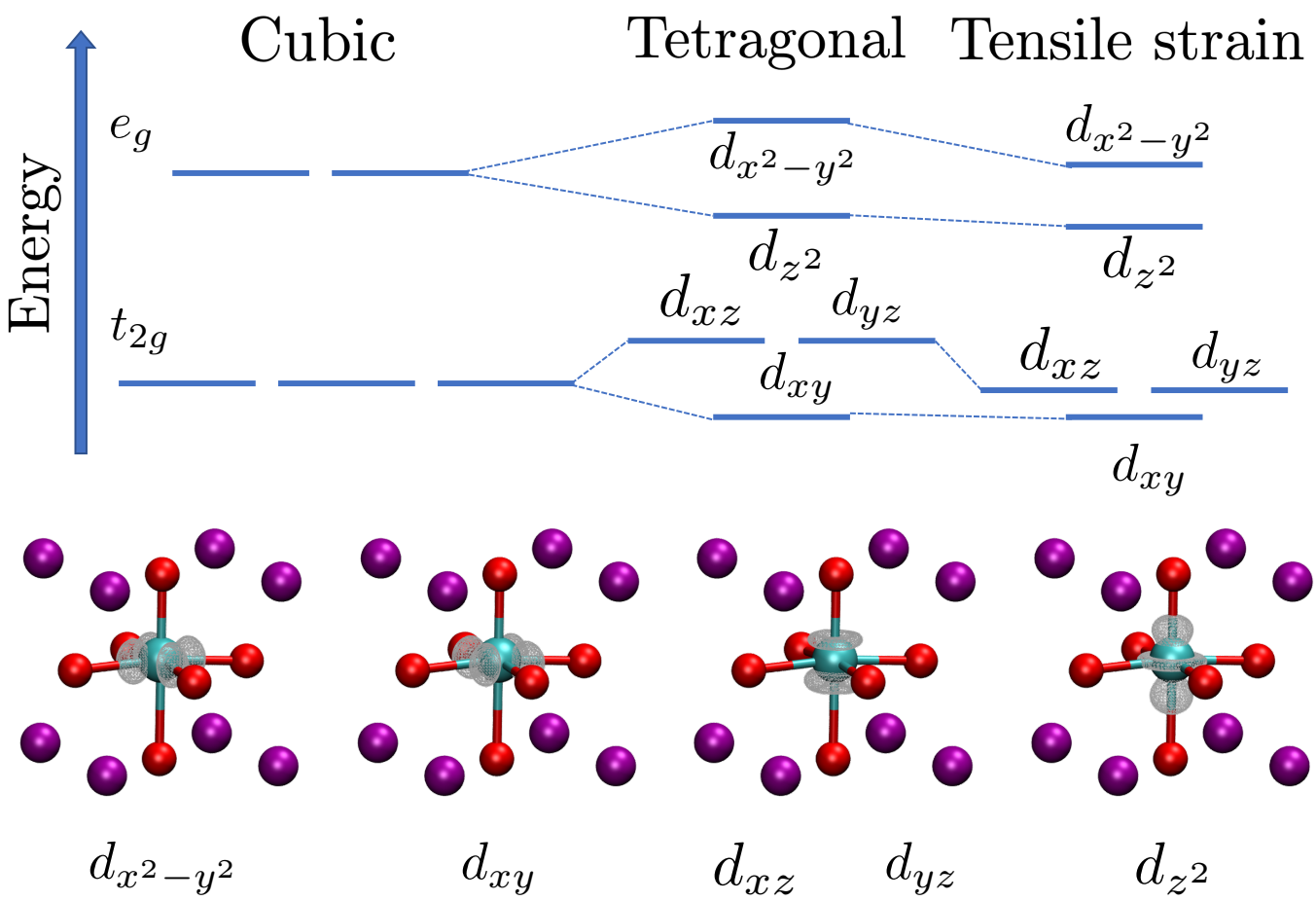

FIG. S2. Upper panel: schematic representation of Nb 4*d* orbitals splitting on a cubic (left), tetragonal (center) and tensile strained tetragonal perovskite. Bottom panel: partial electron density of the first 5 unoccupied states at Γ.

S4. SUBSTRATES LIST

TABLE S2: Substrate list for $KNbO_3$ including Pearson symbol, space group number, lattice misfits, supercell generator matrices, interface band gap (E_g) in eV and junction type.

Formula	Pearson	S.G.#	Plane	ϵ_a	ϵ_b	ϵ_α	$\mathbf{M}_{subs}$	$\mathbf{M}_{KNO}$	E_g	junction type
SnO_2	*tI*12	141	(0 0 1)	0.83	0.83	0.00	$\begin{pmatrix} 1 & 0 \\ 0 & 1 \end{pmatrix}$	$\begin{pmatrix} 1 & 0 \\ 0 & 1 \end{pmatrix}$	0	III
NbO_2	*tI*12	141	(0 0 1)	1.22	1.22	0.00	$\begin{pmatrix} 1 & 0 \\ 0 & 1 \end{pmatrix}$	$\begin{pmatrix} 1 & 0 \\ 0 & 1 \end{pmatrix}$	0	III
Ge	*cF*8	227	(1 1 0)	1.27	-4.52	0.00	$\begin{pmatrix} 1 & 0 \\ 0 & 2 \end{pmatrix}$	$\begin{pmatrix} 1 & 0 \\ 0 & 3 \end{pmatrix}$	0	III

Formula	Pearson	S.G.#	Plane	ϵ_a	ϵ_b	ϵ_α	$\mathbf{M}_{subs}$	$\mathbf{M}_{KNO}$	E_{g}	junction type
CdF_2	$cF12$	225	(1 0 0)	-3.48	-3.48	0.00	$\begin{pmatrix} 1 & 0 \\ 0 & 1 \end{pmatrix}$	$\begin{pmatrix} 1 & 0 \\ 0 & 1 \end{pmatrix}$	0	III
CaF_2	$cF12$	225	(1 0 0)	-3.07	-3.07	0.00	$\begin{pmatrix} 1 & 0 \\ 0 & 1 \end{pmatrix}$	$\begin{pmatrix} 1 & 0 \\ 0 & 1 \end{pmatrix}$	1.85	$\mathrm{I_{tf}}$
Cu_2S	$cF12$	225	(1 0 0)	-2.42	-2.42	0.00	$\begin{pmatrix} 1 & 0 \\ 0 & 1 \end{pmatrix}$	$\begin{pmatrix} 1 & 0 \\ 0 & 1 \end{pmatrix}$	0	III
Na_2O	$cF12$	225	(1 0 0)	-1.68	-1.68	0.00	$\begin{pmatrix} 1 & 0 \\ 0 & 1 \end{pmatrix}$	$\begin{pmatrix} 1 & 0 \\ 0 & 1 \end{pmatrix}$	0	III
HgF_2	$cF12$	225	(1 0 0)	-0.67	-0.67	0.00	$\begin{pmatrix} 1 & 0 \\ 0 & 1 \end{pmatrix}$	$\begin{pmatrix} 1 & 0 \\ 0 & 1 \end{pmatrix}$	0	III
Li_2S	$cF12$	225	(1 0 0)	0.54	0.54	0.00	$\begin{pmatrix} 1 & 0 \\ 0 & 1 \end{pmatrix}$	$\begin{pmatrix} 1 & 0 \\ 0 & 1 \end{pmatrix}$	0	III
SrF_2	$cF12$	225	(1 0 0)	3.08	3.08	0.00	$\begin{pmatrix} 1 & 0 \\ 0 & 1 \end{pmatrix}$	$\begin{pmatrix} 1 & 0 \\ 0 & 1 \end{pmatrix}$	2.50	$\mathrm{I_{tf}}$
KF	$cF8$	225	(0 0 1)	-4.69	-4.69	0.00	$\begin{pmatrix} 1 & 0 \\ 0 & 1 \end{pmatrix}$	$\begin{pmatrix} 1 & 0 \\ 0 & 1 \end{pmatrix}$	1.27	$\mathrm{I_{tf}}$
MgSe	$cF8$	225	(0 0 1)	-3.16	-3.16	0.00	$\begin{pmatrix} 1 & 0 \\ 0 & 1 \end{pmatrix}$	$\begin{pmatrix} 1 & 0 \\ 0 & 1 \end{pmatrix}$	1.67	$\mathrm{II_{tf}}$
LiBr	$cF8$	225	(0 0 1)	-3.12	-3.12	0.00	$\begin{pmatrix} 1 & 0 \\ 0 & 1 \end{pmatrix}$	$\begin{pmatrix} 1 & 0 \\ 0 & 1 \end{pmatrix}$	1.81	$\mathrm{II_{tf}}$
BaO	$cF8$	225	(0 0 1)	-1.33	-1.33	0.00	$\begin{pmatrix} 1 & 0 \\ 0 & 1 \end{pmatrix}$	$\begin{pmatrix} 1 & 0 \\ 0 & 1 \end{pmatrix}$	1.24	$\mathrm{II_{tf}}$
AgCl	$cF8$	225	(0 0 1)	-1.20	-1.20	0.00	$\begin{pmatrix} 1 & 0 \\ 0 & 1 \end{pmatrix}$	$\begin{pmatrix} 1 & 0 \\ 0 & 1 \end{pmatrix}$	1.61	$\mathrm{I_{tf}}$
GeSe	$cF8$	225	(0 0 1)	-0.44	-0.44	0.00	$\begin{pmatrix} 1 & 0 \\ 0 & 1 \end{pmatrix}$	$\begin{pmatrix} 1 & 0 \\ 0 & 1 \end{pmatrix}$	0.71	$\mathrm{I_{sub}}$
TlF	$cF8$	225	(0 0 1)	-0.17	-0.17	0.00	$\begin{pmatrix} 1 & 0 \\ 0 & 1 \end{pmatrix}$	$\begin{pmatrix} 1 & 0 \\ 0 & 1 \end{pmatrix}$	1.89	$\mathrm{I_{tf}}$
NaCl	$cF8$	225	(0 0 1)	0.02	0.02	0.00	$\begin{pmatrix} 1 & 0 \\ 0 & 1 \end{pmatrix}$	$\begin{pmatrix} 1 & 0 \\ 0 & 1 \end{pmatrix}$	1.83	$\mathrm{I_{tf}}$
KH	$cF8$	225	(0 0 1)	0.10	0.10	0.00	$\begin{pmatrix} 1 & 0 \\ 0 & 1 \end{pmatrix}$	$\begin{pmatrix} 1 & 0 \\ 0 & 1 \end{pmatrix}$	1.63	$\mathrm{II_{tf}}$

Formula	Pearson	S.G.#	Plane	ϵ_a	ϵ_b	ϵ_α	$\mathbf{M}_{subs}$	$\mathbf{M}_{KNO}$	E_{g}	junction type
CaS	$cF8$	225	(0 0 1)	0.45	0.45	0.00	$\begin{pmatrix} 1 & 0 \\ 0 & 1 \end{pmatrix}$	$\begin{pmatrix} 1 & 0 \\ 0 & 1 \end{pmatrix}$	0.60	$\mathrm{II_{tf}}$
RbF	$cF8$	225	(0 0 1)	0.85	0.85	0.00	$\begin{pmatrix} 1 & 0 \\ 0 & 1 \end{pmatrix}$	$\begin{pmatrix} 1 & 0 \\ 0 & 1 \end{pmatrix}$	1.79	$\mathrm{I_{tf}}$
YSe	$cF8$	225	(0 0 1)	1.61	1.61	0.00	$\begin{pmatrix} 1 & 0 \\ 0 & 1 \end{pmatrix}$	$\begin{pmatrix} 1 & 0 \\ 0 & 1 \end{pmatrix}$	0	III
SnAs	$cF8$	225	(0 0 1)	2.08	2.08	0.00	$\begin{pmatrix} 1 & 0 \\ 0 & 1 \end{pmatrix}$	$\begin{pmatrix} 1 & 0 \\ 0 & 1 \end{pmatrix}$	0	III
YAs	$cF8$	225	(0 0 1)	2.56	2.56	0.00	$\begin{pmatrix} 1 & 0 \\ 0 & 1 \end{pmatrix}$	$\begin{pmatrix} 1 & 0 \\ 0 & 1 \end{pmatrix}$	0	III
AgBr	$cF8$	225	(0 0 1)	2.83	2.83	0.00	$\begin{pmatrix} 1 & 0 \\ 0 & 1 \end{pmatrix}$	$\begin{pmatrix} 1 & 0 \\ 0 & 1 \end{pmatrix}$	1.68	$\mathrm{II_{tf}}$
SnS	$cF8$	225	(0 0 1)	2.83	2.83	0.00	$\begin{pmatrix} 1 & 0 \\ 0 & 1 \end{pmatrix}$	$\begin{pmatrix} 1 & 0 \\ 0 & 1 \end{pmatrix}$	0.25	$\mathrm{II_{tf}}$
LaS	$cF8$	225	(0 0 1)	3.30	3.30	0.00	$\begin{pmatrix} 1 & 0 \\ 0 & 1 \end{pmatrix}$	$\begin{pmatrix} 1 & 0 \\ 0 & 1 \end{pmatrix}$	0	III
CaSe	$cF8$	225	(0 0 1)	4.81	4.81	0.00	$\begin{pmatrix} 1 & 0 \\ 0 & 1 \end{pmatrix}$	$\begin{pmatrix} 1 & 0 \\ 0 & 1 \end{pmatrix}$	0.17	$\mathrm{II_{tf}}$
TlF	$cF8$	225	(1 1 0)	-0.16	-0.16	0.00	$\begin{pmatrix} 1 & 0 \\ 0 & 1 \end{pmatrix}$	$\begin{pmatrix} 1 & 0 \\ 0 & 1 \end{pmatrix}$	1.89	$\mathrm{I_{tf}}$
RbF	$cF8$	225	(1 1 0)	0.85	-4.92	0.00	$\begin{pmatrix} 1 & 0 \\ 0 & 2 \end{pmatrix}$	$\begin{pmatrix} 1 & 0 \\ 0 & 3 \end{pmatrix}$	2.12	$\mathrm{I_{tf}}$
RbF	$cF8$	225	(1 1 0)	0.85	-4.92	0.00	$\begin{pmatrix} 4 & 0 \\ 0 & 1 \end{pmatrix}$	$\begin{pmatrix} 3 & 0 \\ 0 & 1 \end{pmatrix}$	2.12	$\mathrm{I_{tf}}$
LiF	$cF8$	225	(1 1 0)	1.48	-4.33	0.00	$\begin{pmatrix} 4 & 0 \\ 0 & 1 \end{pmatrix}$	$\begin{pmatrix} 1 & 0 \\ 0 & 3 \end{pmatrix}$	1.97	$\mathrm{I_{tf}}$
YSe	$cF8$	225	(1 1 0)	1.61	-4.20	0.00	$\begin{pmatrix} 1 & 0 \\ 0 & 2 \end{pmatrix}$	$\begin{pmatrix} 1 & 0 \\ 0 & 3 \end{pmatrix}$	0	III
YSe	$cF8$	225	(1 1 0)	1.61	-4.20	0.00	$\begin{pmatrix} 1 & 0 \\ 0 & 2 \end{pmatrix}$	$\begin{pmatrix} 3 & 0 \\ 0 & 1 \end{pmatrix}$	0	III
SnAs	$cF8$	225	(1 1 0)	2.08	-3.75	0.00	$\begin{pmatrix} 1 & 0 \\ 0 & 2 \end{pmatrix}$	$\begin{pmatrix} 3 & 0 \\ 0 & 1 \end{pmatrix}$	0	III

Formula	Pearson	S.G.#	Plane	ϵ_a	ϵ_b	ϵ_α	$\mathbf{M}_{subs}$	$\mathbf{M}_{KNO}$	E_{g}	junction type
YAs	$cF8$	225	(1 1 0)	2.56	-3.31	0.00	$\begin{pmatrix} 1 & 0 \\ 0 & 2 \end{pmatrix}$	$\begin{pmatrix} 1 & 0 \\ 0 & 3 \end{pmatrix}$	0	III
AgBr	$cF8$	225	(1 1 0)	2.83	-3.05	0.00	$\begin{pmatrix} 1 & 0 \\ 0 & 2 \end{pmatrix}$	$\begin{pmatrix} 3 & 0 \\ 0 & 1 \end{pmatrix}$	1.65	$\mathrm{I_{sub}}$
SnS	$cF8$	225	(1 1 0)	2.83	-3.05	0.00	$\begin{pmatrix} 1 & 0 \\ 0 & 2 \end{pmatrix}$	$\begin{pmatrix} 3 & 0 \\ 0 & 1 \end{pmatrix}$	1.07	$\mathrm{II_{tf}}$
LaS	$cF8$	225	(1 1 0)	3.30	-2.61	0.00	$\begin{pmatrix} 1 & 0 \\ 0 & 2 \end{pmatrix}$	$\begin{pmatrix} 1 & 0 \\ 0 & 3 \end{pmatrix}$	0	III
ZnS	$hP4$	186	(1 1 0)	-4.37	4.66	0.00	$\begin{pmatrix} 3 & 0 \\ 0 & 1 \end{pmatrix}$	$\begin{pmatrix} 1 & 0 \\ 0 & 2 \end{pmatrix}$	1.91	$\mathrm{II_{sub}}$
LaN	$hP4$	186	(1 1 0)	2.71	-1.26	0.00	$\begin{pmatrix} 1 & 0 \\ 0 & 3 \end{pmatrix}$	$\begin{pmatrix} 2 & 0 \\ 0 & 1 \end{pmatrix}$	0.41	$\mathrm{II_{tf}}$
BeO	$hP4$	186	(1 1 0)	-4.97	0.80	0.00	$\begin{pmatrix} 3 & 0 \\ 0 & 1 \end{pmatrix}$	$\begin{pmatrix} 2 & 0 \\ 0 & 1 \end{pmatrix}$	2.55	$\mathrm{II_{tf}}$
ZnSe	$hP4$	186	(1 1 0)	0.91	-4.86	0.00	$\begin{pmatrix} 1 & 0 \\ 0 & 2 \end{pmatrix}$	$\begin{pmatrix} 3 & 0 \\ 0 & 1 \end{pmatrix}$	1.65	$\mathrm{I_{tf}}$
GaAs	$hP4$	186	(1 1 0)	1.04	-4.73	0.00	$\begin{pmatrix} 1 & 0 \\ 0 & 2 \end{pmatrix}$	$\begin{pmatrix} 1 & 0 \\ 0 & 3 \end{pmatrix}$	0.87	$\mathrm{I_{sub}}$
CdS	$hP4$	186	(1 1 0)	4.39	-1.57	0.00	$\begin{pmatrix} 1 & 0 \\ 0 & 2 \end{pmatrix}$	$\begin{pmatrix} 3 & 0 \\ 0 & 1 \end{pmatrix}$	1.35	$\mathrm{II_{sub}}$

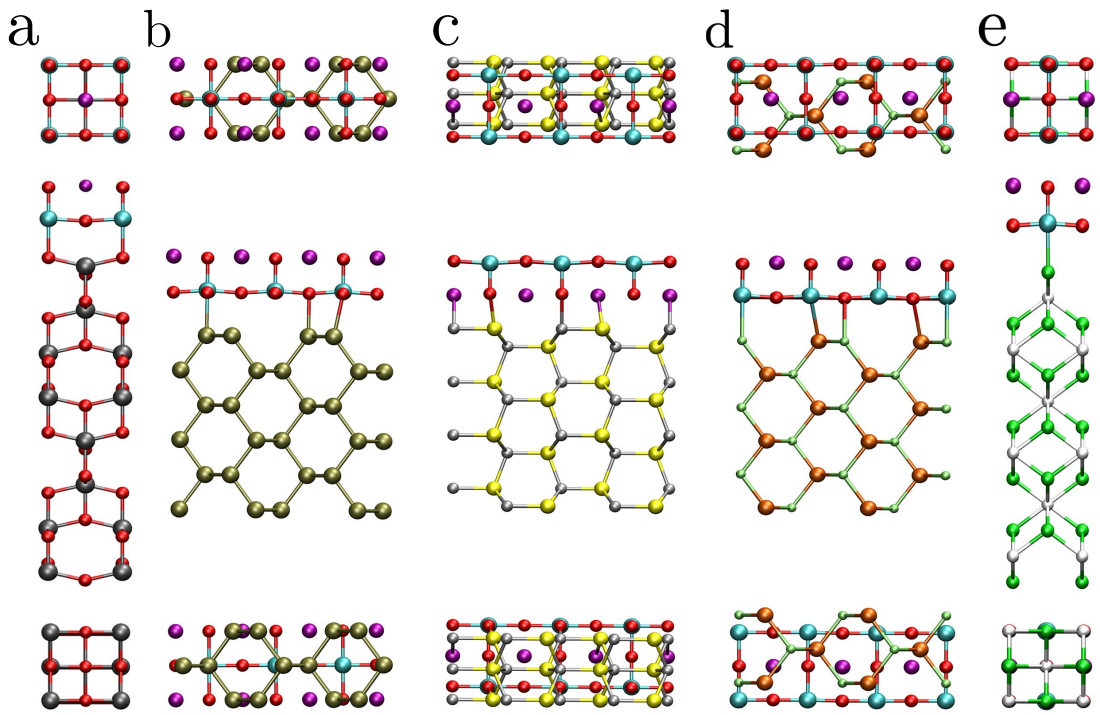

FIG. S3. Top, side and bottom view of interfaces models for the epitaxial growth of $KNbO_3$ thin-films with different prototypes: **a**) anatase, **b**) diamond, **c**) zincblende, **d**) wurtzite and **e**) fluorite. Colors: K, purple; Nb, cyan; O, red; Sn, gray; Ge, tan ; Zn, silver; S, yellow; Ga, orange; As, light green; Ca, white; F, green.

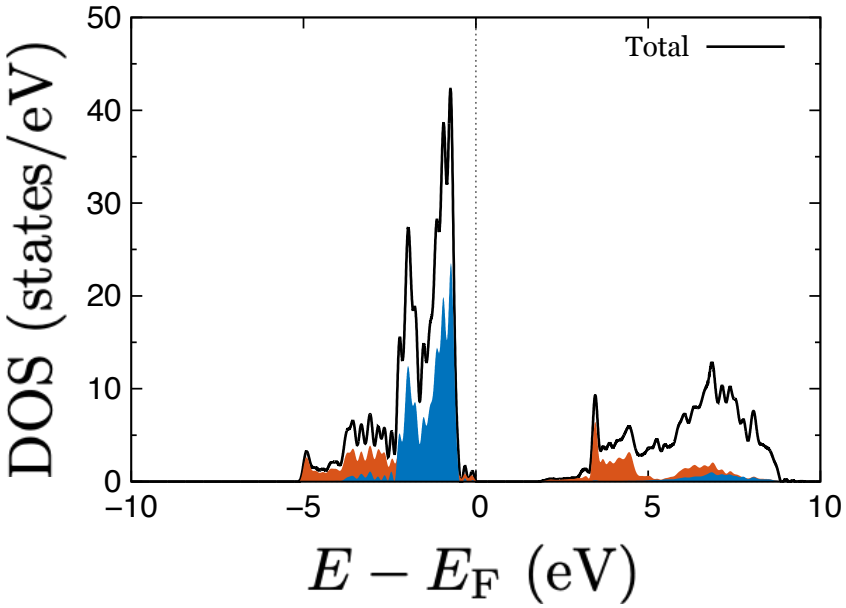

FIG. S4. Density of states, DOS, for the $KNbO_3$/NaCl interface. Total DOS is shown with solid black line and $KNbO_3$ and NaCl DOS projections are coloured on orange and blue areas respectively.

S5. I_{tf} JUNCTIONS

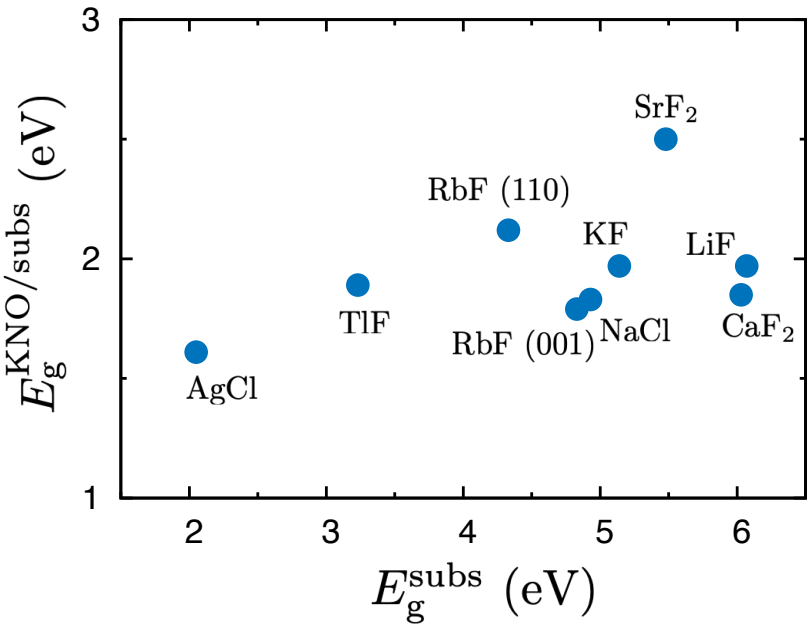

FIG. S5. Correlation between $KNbO_3$/substrate band gaps, $E_g^{KNO/subs}$, and substrate band gaps, E_g^{subs}, for I_{tf} heterojuntions.

S6. $KNBO_3$ RECONSTRUCTION

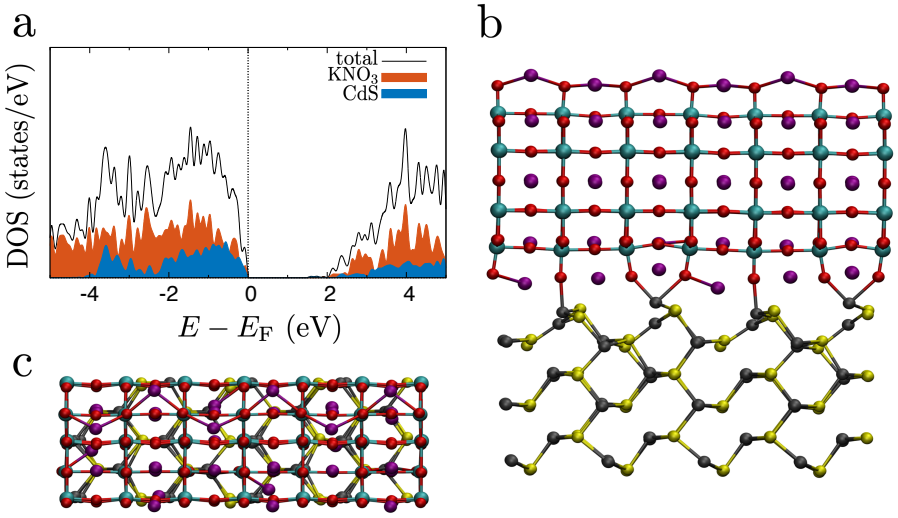

FIG. S6. **a**) Density of states, DOS, for the reconstructed $KNbO_3$/CdS interface. **b**) Side and **c**) top view of interfaces models for epitaxial growth of reconstructed $KNbO_3$ (001) thin-films on top of CdS.

S7. $KNBO_3$ SPECTRA

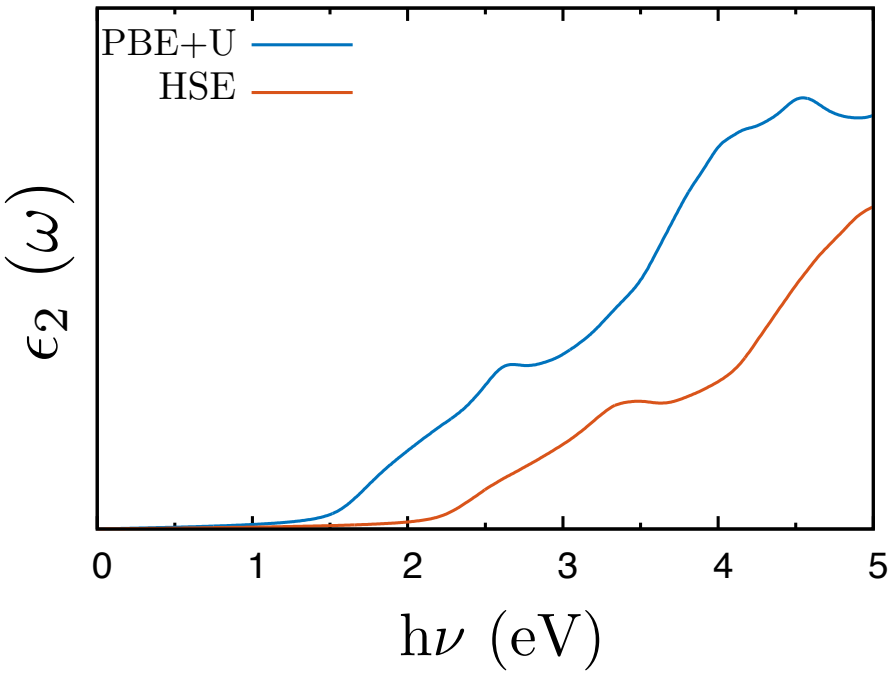

FIG. S7. Imaginary part of the frequency-dependent dielectric function, $\epsilon_2\ (\omega)$, for the $KNbO_3$/CdS using PBE+U (blue) and HSE (orange) functional.

[1] J. W. S. Cassels, *An introduction to the Geometry of Numbers* (Springer, Berlin, 1959), 1 edn.

[2] F. Schmidt, M. Landmann, E. Rauls, N. Argiolas, S. Sanna, W. G. Schmidt, and A. Schindlmayr, *Consistent Atomic Geometries and Electronic Structure of Five Phases of Potassium Niobate from Density-Functional Theory*, Adv. Mater. Sci. Eng. p. 3981317 (2017).

[3] M. D. Fontana, G. Metra, J. L. Servoin, and F. Gervais, *Infrared spectroscopy in $KNbO_3$ through the successive ferroelectric phase transitions*, J. Phys. C: Solid State Phys **17**, 483–514 (1984).

[4] F. Wang, I. Grinberg, and A. Rappe, *Semiconducting ferroelectric photovoltaics through Zn^{2+} doping into $KNbO_3$ and polarization rotation*, Phys. Rev. B **89**, 235105 (2014).

[5] S. Cabuk, *Electronic structure and optical properties of $KNbO_3$: First principles study*, J. Optoelectron. Adv. M. **3**, 100–107 (2007).

[6] T. Zhang, K. Zhao, J. Yu, J. Jin, Y. Qi, H. Li, X. Hou, and G. Liu, *Photocatalytic water splitting for hydrogen generation on cubic, orthorhombic, and tetragonal $KNbO_3$ microcubes*, Nanoscale **5**, 8375–8383 (2013).

[7] Y. Shiozaki, E. Nakamura, and T. Mitsui, *Ferroelectrics and Related Substances: Oxides Part 1: Perovskite-Type Oxides and $LiNbO_3$ Family* (Springer, Landolt-Bornstein, 2001), 1 edn.